

1 High-resolution Carbon cycling data from 2019 to 2021 measured at six 2 Austrian Long-Term Ecosystem Research sites

3

4 Thomas Dirnböck^{1*}, Michael Bahn², Eugenio Diaz-Pines³, Ika Djukic¹, Michael Englisch⁴, Karl Gartner⁴,
5 Günther Gollobich⁴, Armin Malli⁴, Johannes Ingrisich², Barbara Kitzler⁴, Karl Knaebel¹, Johannes
6 Kobler¹, Andreas Maier⁵, Christoph Wohner¹, Ivo Offenthaler¹, Johannes Peterseil¹, Gisela Pröll¹,
7 Sarah Venier¹, Sophie Zechmeister-Boltenstern³, Anita Zolles⁴, Stephan Glatzel⁵

8

9 ¹ Environment Agency Austria, Spittelauer Lände 5, A-1090 Vienna, Austria

10 ² Department of Ecology, Universität Innsbruck, Innsbruck, Austria; Innrain 52, 6020 Innsbruck

11 ³ Institute of Soil Research, Department of Forest- and Soil Sciences, BOKU University. Peter-Jordan-
12 Straße 82, 1190 Vienna, Austria

13 ⁴ Austrian Research Centre for Forests, Seckendorff-Gudent Weg 8, 1131 Vienna, Austria

14 ⁵ Department of Geography and Regional Research, Faculty of Earth Sciences, Geography and
15 Astronomy, University of Vienna, Josef-Holaubek-Platz 2, 1090 Vienna, Austria

16 *corresponding author: Thomas Dirnböck; thomas.dirnboeck@umweltbundesamt.at

17

18 Abstract

19 Seven long-term observation sites have been established in six regions across Austria, covering major
20 ecosystem types such as forests, grasslands and wetlands across a wide bioclimatic range. The
21 purpose of these observations is to measure key ecosystem parameters serving as baselines for
22 assessing the impacts of extreme climate events on the carbon cycle. The data sets collected include
23 meteorological variables, soil microclimate, CO₂ fluxes and tree stem growth, all recorded at high
24 temporal resolution (15 – 60 minutes) between 2019 and 2021 (including one year of average
25 climate conditions and two comparatively dry years). The DOIs of the dataset can be found in the
26 data availability chapter. The sites will be integrated into the European Research Infrastructure for
27 Integrated European Long-Term Ecosystem, Critical Zone, and Socio-Ecological Research (eLTER RI).
28 Subsequently, new data covering the variables presented here will be continuously available through
29 its data integration portal. This step will allow the data to reach its full potential for research on
30 drought-related ecosystem carbon cycling.

31

32 1. Introduction

33 Climate change has been affecting ecosystems globally with strong implications for the terrestrial
34 carbon (C) cycle, which in turn feeds back to the climate system (Heimann and Reichstein, 2008). As
35 an emerging feature of climate change, extreme climatic events (ECEs) are expected to occur with
36 increasing frequency and intensity in the coming decades (IPCC, 2021). ECEs are considered to exert
37 stronger impacts on ecosystems and the services they provide to mankind than gradual changes in
38 climate (Frank et al., 2015; Reichstein et al., 2013; Grünzweig et al., 2022; Anderegg et al., 2020).
39 Understanding, predicting and managing extreme climate events and their consequences for
40 ecosystems and societies will therefore be one of the big challenges in the coming decades. To detect

41 and attribute impacts of ECEs on ecosystem processes and services they need to be evaluated on the
42 background of the typical interannual range of these processes (Ciais et al., 2005; Bernal et al., 2012;
43 Fu et al., 2020; Schindlbacher et al., 2012) and analyses of ecosystem resilience to ECEs require a
44 robust quantification of baselines of ecosystem functioning (Bahn and Ingrisch, 2018; Ingrisch and
45 Bahn, 2018). For deriving such baselines as well as interannual variability of ecosystem carbon
46 cycling, coordinated and representative observation networks need to be in place to enable data
47 retrieval as well as rapid-response scientific campaigns to study after-effects and post-disturbance
48 trajectories resulting from ECEs (Kulmala, 2018; Mahecha et al., 2017; Mirtl et al., 2018; Dirnböck et
49 al., 2019; Müller and Bahn, 2022). Datasets obtained through such observation networks are also
50 essential for benchmarking models (Futter et al., 2023; Baatz et al., 2021; Wu et al., 2018) and for
51 comparison with ecosystem experiments (Kröel-Dulay et al., 2022).

52 Within a research infrastructure project focusing on ecosystem carbon, nitrogen, and water fluxes
53 (Long-Term Ecosystem Research for Carbon, Water, and Nitrogen (LTER-CWN, [https://www.lter-
54 austria.at/cwn/](https://www.lter-austria.at/cwn/)), we equipped seven long-term observation sites in six regions, which are part of the
55 existing Long-Term Ecological Research Network of Austria (LTER-Austria), with high temporal
56 resolution (30-60 minutes) C cycle measurements. The sites cover three major ecosystem types
57 occurring across Austria (forests, managed mountain grassland, wetlands) and most of them are part
58 of socio-ecological research platforms for transdisciplinary studies (Figure 1). Here, we provide
59 observational ecosystem response data capturing naturally-occurring ECEs from the first three years
60 after the onset of the infrastructure, 2019 to 2021. These data sets include meteorological variables,
61 soil microclimate, CO₂ flux measurements using automated chambers (soil CO₂ efflux) and eddy
62 covariance techniques (net ecosystem exchange), respectively, and tree stem radial increments and
63 shrinkage in forested plots.

64

65 2. Site descriptions

66 The sites are key research infrastructures for ecosystem-related greenhouse gas observations in
67 Austria. They include forests (Klausen-Leopoldsdorf and Rosalia in Lower Austria, Zöbelboden in
68 Upper Austria, and Stubai in Tyrol), mountain grassland (Stubai, Tyrol), and wetlands (Pürgschachen
69 Moor, Styria and Lake Neusiedl reed belt, Burgenland). This network of sites covers typical forest,
70 alpine and wetland ecosystems of Central Europe (Figure 1). Furthermore, the sites represent
71 different geological characteristics, from crystalline rock in the central Alps to the limestone in the
72 northern Alps to unconsolidated Holocene sediments in lowlands. All sites are part of the Austrian
73 LTER network and, once officially launched, will be included in the European eLTER research
74 infrastructure (<https://elter-ri.eu/>). For a detailed description of the sites, we refer to the Dynamic
75 Ecological Information Management System - Site and dataset registry (DEIMS-SDR) (Table 1).

76 2.1. Rosalia Forest Demonstration Centre (Mixed beech forest)

77 The Rosalia Forest Demonstration Centre was settled in 1972, as a cooperation between the BOKU
78 University, Vienna, Austria, and the Austrian Federal Forests, and has approximately 1000 ha in the
79 western slopes of the Rosalia Mountains (Rosaliengebirge) in Lower Austria (Figure 1, Table 1). The
80 forest hosts all major tree species occurring in Austria, i.e. European beech (*Fagus sylvatica* L.),
81 Norway spruce (*Picea abies* (L.) H.Karst.), Scots pine (*Pinus sylvestris* L.), Larch (*Larix decidua* Mill.),
82 and Fir (*Abies alba* Mill.). The altitude ranges from 320 to 725 m a.s.l., and mean annual temperature
83 and mean annual precipitation are 6.5 °C and 796 mm, respectively. Substrate is mainly composed by
84 crystalline rocks, and soils are predominantly cambisols (Working Group WRB 2015); sporadically in

85 combination with planosols (in plains and moderate slopes), with fluvisols (in valleys) or podzolic
86 cambisols (steep slopes) (Fürst et al., 2021).

87 The demonstration forest holds several experimental and observation sites distributed along its area,
88 including water, soil, vegetation and air observations (e.g. Gillespie et al., 2023). A watershed (220
89 ha) is subject to hydrological observations (Fürst et al., 2021), and the forest is regularly monitored
90 on permanent plots (Gollob et al., 2020). The meteorological data presented here originates from
91 three stations located at 385 (Mehlbeerleiten), 500 (Kuhwald) and 640 m a.s.l. (Heuberg). The C cycle
92 data was measured on a long-term experimental site launched in 2012. The site is located in a pure
93 mature beech stand at 600 m a.s.l. (47° 42' 26" N; 16° 17' 59" E). It faces north-west, with a slope of
94 approximately 20 %. This experiment focuses on investigating the effect of changing precipitation
95 patterns for selected soil biogeochemical and microbiological processes (Leitner et al., 2017; Liu et
96 al., 2019; Schwen et al., 2015; Gillespie et al., 2024). Monitoring is performed on control and on
97 manipulated plots. The data from both natural and manipulated plots is published with this paper.
98 Manipulation involves the use of rain-out-shelters (for simulating drought periods of different length)
99 and of an irrigation system (for recreating rainfall events of different intensity). The monitoring
100 infrastructure involves the measurements of greenhouse gases (GHG) (N₂O, CH₄ and CO₂) fluxes, soil
101 nutrients (suction cups) and microclimate parameters.

102 2.2. Klausen-Leopoldsdorf (Beech forest)

103 The site, Klausen-Leopoldsdorf, is located about 40 km south-west of Vienna on a NNE-facing slope
104 and was founded in the 1990s as one of Austria's site contributing to the International Co-operative
105 Programme on Assessment and Monitoring of Air Pollution Effects on Forests (ICP Forests) (Neumann
106 and Starlinger, 2001). The site is divided into four different sub-areas within a small catchment: 1)
107 the ICP Forests site, 2) a weather station, located 2.7 km from the ICP Forests intensive plots at 398
108 m a.s.l., 3) a catchment runoff weir (475 m a.s.l.), and 4) the LTER-CWN measurement plot (520 m
109 a.s.l.), where the C-cycle data presented here was measured (Figure 1, Table 1). The forest within the
110 measurement plot is a pure beech (*Fagus sylvatica* L.) stand. The mean annual temperature is 8°C,
111 mean annual precipitation is 801 mm (2010-2022). The geological substrate is sandstone, the soil
112 type is mainly stagnic cambisol/dystric cambisol (Working Group WRB 2015). Instruments installed
113 on the LTER-CWN measurement area include a sap flow and dendrometer measurement system on
114 10 trees, 12 GHG automated measurement chambers for CO₂ respiration, soil moisture and soil
115 temperature sensors in different soil depths (5 – 30 cm).

116 In addition to the data presented here, many other data sets are available. Soil GHG fluxes (manual
117 sampling) were measured starting in the year 2001 (Kitzler et al., 2006). On the ICP Forests site,
118 instruments for long-term monitoring (since 1996) such as soil moisture, air temperature and relative
119 humidity, soil temperature, soil solution with suction cups, throughfall deposition, litterfall traps,
120 stemflow, and manual and automatic dendrometers are installed and the data is available under
121 <https://bfw.ac.at/lims/level2.daten> or via the ICP Forests Program Centre.

122 2.3. Lake Neusiedl (reed belt)

123 The measurement site is located in the eastern reed belt of the lake and as such inside the National
124 Park Lake Neusiedl - Seewinkel (Figure 1, Table 1). The region (average altitude: 120 m.a.s.l.) is
125 characterized by a (sub)-continental Pannonian climate with a mean annual precipitation of 576 mm
126 (2013-2022). The reed belt is a dynamic ecosystem consisting of a mosaic of reed stocks (*Phragmites*
127 *australis* (Cav.) Trin. ex Steud.), sediment and open water areas. Increasing dry periods and thus
128 successive drying of the reed belt since 2018 have led to an increase in reed stocks within the belt, as
129 well as an increase in sediment areas and a strong decline in open water areas, according to a 2021

130 study that investigated the spatial and temporal variations within the reed ecosystem at Lake
131 Neusiedl (Buchsteiner et al., 2023). Processes driving CH₄ emissions from the reed belt have recently
132 been investigated in detail (Baur et al., 2024).

133 The data presented here stems from devices permanently installed on site. They include an eddy
134 covariance tower for CO₂, CH₄ and water vapor fluxes and relevant accompanying meteorological
135 parameters as well as soil heat flux, soil moisture, and soil temperature sensors.

136 2.4. Pürgschachen Moor (peat bog)

137 The Pürgschachen Moor is located on the bottom of the Styrian Enns valley at an altitude of 632 m
138 a.s.l. (Figure 1, Table 1). It is a pine peat bog with an extent of about 62 ha. Thus, it is the largest (to a
139 large part) intact valley peat bog in Austria with a closed peat moss cover and a good example of the
140 formerly widely distributed peatlands of inner-alpine valleys of the European Alps. The mean average
141 temperature is 8.2 °C and mean annual precipitation is 1233 mm (2013-2022). The typical vegetation
142 of the peat bog is constituted of three associations of plants *Pino mugo-Sphagnetum magellanici*
143 (pine peat bog association), *Sphagnetum magellanici* (coloured bog moss association), and *Caricetum*
144 *limosae* (bog sedge association), depending on the prevailing hydrological site conditions. The
145 current mean water table depth is about 14 cm below soil surface at the central peat bog area. Peat
146 decomposition and related CO₂ and CH₄ fluxes were subject of a series of research studies (Drollinger
147 et al., 2019; Knierzinger et al., 2020; Müller et al., 2022; Glatzel et al., 2023).

148 The data presented here stems from devices permanently installed roughly in the center of the peat
149 bog. They include an eddy covariance tower for CO₂, CH₄ and water vapor fluxes and relevant
150 accompanying meteorological parameters as well as soil heat flux, soil moisture, and soil
151 temperature sensors.

152 2.5. Stubai (subalpine hay meadow, Larch and Spruce forest)

153 The two observation plots used in this study are part of the LTER Site Stubai (Table 1), which is
154 located in the Stubai Alps in Tyrol, Austria (Figure 1). Research at the study site was established in
155 1993. The two observation plots are a mountain grassland and a subalpine forest at an alpine pasture
156 area called "Kaserstattalm". The underlying rock is siliceous and calcareous. The average air
157 temperature is about 3°C and the precipitation approx. 1100 mm. About 35% of the annual
158 precipitation occurs as snow during winter months.

159 The grassland site is located at an altitude of 1810 -1850 m a.s.l on a south-east facing slope with an
160 inclination of ca. 20°. The site is an extensively managed meadow that is harvested once a year in
161 early August and grazed lightly in late summer. The soil is a dystric cambisol (Working Group WRB
162 2015). The vegetation type is a *Trisetetum flavescens* and consists of perennials grasses and forbs
163 dominated by *Agrostis capillaris* L., *Festuca rubra* L., *Anthoxanthum odoratum* L., *Ranunculus*
164 *montanus* Willd., *Leontodon hispidus* L., *Trifolium repens* L. and *T. pratense* L. (Bahn et al., 2009;
165 Schmitt et al., 2010).

166 The forested observation plot is located close to the tree line at 1960 m a.s.l. on a slope with an
167 inclination of 20-35°. It is dominated by the two common tree species European larch (*Larix decidua*
168 Mill.) and Norway spruce (*Picea abies* (L.) H.Karst.). In former years, the plot was a pasture and it was
169 reforested in the 1980s (Oberleitner et al., 2022).

170 Both observation plots are equipped with micrometeorological stations, soil environment monitoring
171 (soil moisture, soil temperature), and soil CO₂ devices. At both observation plots, we measured soil
172 CO₂ fluxes with automated chambers during the summer. The forest plot is additionally equipped
173 with tree dendrometers and tree sapflow sensors. In the grassland, land use and drought related

174 carbon cycle research was carried out over the last two decades (Fuchslueger et al., 2014; Hasibeder
175 et al., 2015; Ingrisch et al., 2020; Ingrisch et al., 2018). Research using the forest plot started only
176 recently (Oberleitner et al., 2022).

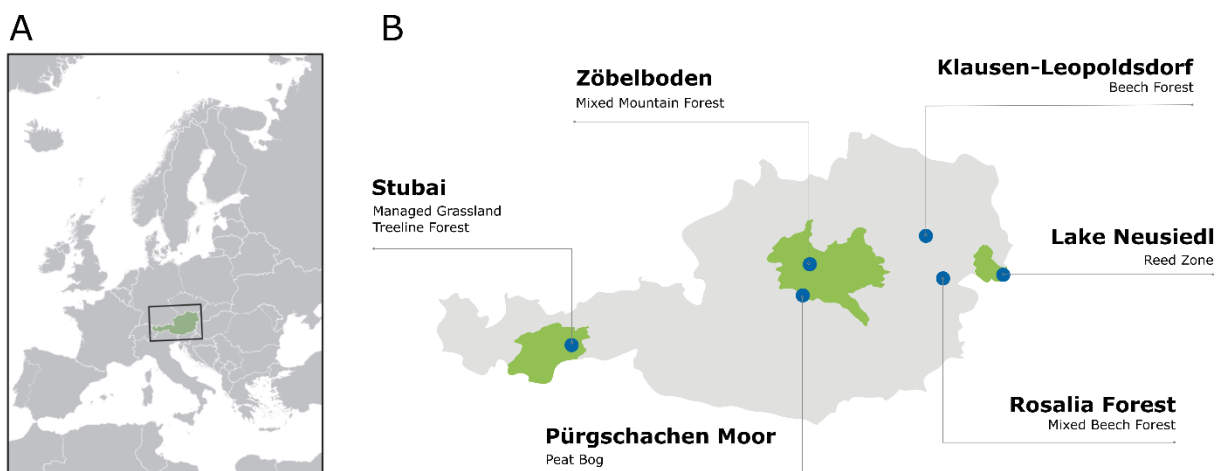
177 2.6. Zöbelboden (mixed Beech forest)

178 The site LTER Zöbelboden is located in the National Park Kalkalpen in the Northern Limestone Alps,
179 Austria (Figure 1). The measurements were established in 1992 as part of the International Cooperative
180 Programme on Integrated Monitoring of Air Pollution Effects on Ecosystems (ICP IM) covering a 90 ha
181 catchment with an elevation range of 550 to 956 m a.s.l. (Table 1). The main underlying rock type is
182 Norian dolomite (*Hauptdolomit*), partly overlain by limestone (*Plattenkalk*). According to long-term
183 meteorological measurements (1993-2022), mean annual air temperature and precipitation are 8.2 °C
184 and 1645 mm, respectively. Maximum precipitation occurs in summer and snowfall usually between
185 December and April.

186 The data presented here was measured at the Intensive Plot II situated on a steep (36° on average)
187 north-westerly exposed slope at 880 m a.s.l. The soils of the plot are lithic and rendzic leptosols
188 (Working Group WRB 2015). The plot is dominated by beech (*Fagus sylvatica* L.) with intermixed
189 sycamore (*Acer pseudoplatanus* L.), European ash (*Fraxinus excelsior* L.) and spruce (*Picea abies* (L.)
190 H.Karst.). Since the year 1995, this plot is equipped with a number of field measurement devices for
191 long-term monitoring (throughfall deposition, litter fall traps, lysimeters, soil moisture and
192 temperature sensors, manual dendrometers) and supplemented by other monitoring activities (tree
193 inventory, needle and leave chemistry, soil chemistry, etc.; see e.g. Leitner et al., 2020; Kobler et al.,
194 2019; Dirnböck et al., 2016; Dirnböck et al., 2020). Drought-impacts on carbon allocation in the
195 forests of the catchment is currently one of the research foci for which long-term observation data
196 exists (see e.g. Hartl-Meier et al., 2014) as well as experimental plots with rainout shelters.

197 The instruments and data included here are soil respiration automated chambers, soil water
198 potential and temperature sensors as well as automated dendrometers. The meteorological data
199 stems from a station in close proximity at the plateau at 890 m a.s.l.. The site is also equipped with
200 an Eddy covariance tower, but this data will be published elsewhere.

201



202

203 *Figure 1.* Location of sites in A) Europe and B) Austria. Blue dots indicate the sites; green areas are long-term socio-
204 ecological research platforms (LTSER) (from left to right: LTSER Tyrolian Alps, LTSER Eisenwurzen, and LTSER Lake Neusiedl)
205 within the LTER Austria network.

Table 1. Metadata of the sites and observation plots. Geographic boundaries, linked data sets, etc. can be found in the site and dataset registry system DEIMS-SDR.

Site (Ecosystem type)	Site Code	Altitude (m a.s.l.)	Annual temperature (°C)	Annual precipitation (mm)	Observation plot	DEIMS.iD
Rosalia Forest Demonstration Centre (mixed beech forest)	ROS	600	6.5	796		https://deims.org/77c127c4-2ebe-453b-b5af-61858ff02e31
					Heuberg Meteorological Station	https://deims.org/locations/44854b32-64c3-4c9d-9aec-9b0b74f8ac70
					Kuhwald Meteorological Station	https://deims.org/locations/1225d57e-02da-47fd-9760-ab39d64999ef
					Mehlbeerleiten Meteorological Station	https://deims.org/locations/0becf0ce-98d7-4f64-a074-f89046083e5e
				Experimental Station	https://deims.org/locations/b7008603-fca2-452f-9b3d-aad30cdfc7a	
Klausen-Leopoldsdorf (beech forest)	KLL	520	8	801	Measuring station	https://deims.org/bb472a51-f85f-4de0-8358-f21ecbe2a102 https://deims.org/locations/d5cba3ce-7489-46d1-8d97-61641ffb5758
Lake Neusiedl (reed zone)	NSS	120	11.5	576	Same as site	https://deims.org/locations/4234987b-9031-4332-9bdd-f869d503ac51
Pürgschachen Moor (peat bog)	PUE	632	8.2	1233	Same as site	https://deims.org/locations/ab2d021b-f318-487a-a85b-ab34566e4c02
Stubai (managed grassland)	KAS	1830	3	1100	Kaserstattalm meadow	https://deims.org/324f92a3-5940-4790-9738-5aa21992511c https://deims.org/locations/cf7843b7-32d6-44e9-ba82-9a8d915036a7

1960

Kaserstattalm forest

<https://deims.org/locations/af2afdad-d6fb-4580-b6e3-be7d07b56f8e>

Zöbelboden (mixed mountain forest)

ZOE 880 8.2 1645

Intensive Plot II

<https://deims.org/8eda49e9-1f4e-4f3e-b58e-e0bb25dc32a6>
<https://deims.org/locations/bc96a499-1b20-4da8-be2d-17306d64b788>

208

209 3. Dataset description, measuring methods, QA/QC

210 We followed routine quality assurance (QA) and quality control (QC) procedures to ensure
 211 functionality of the sensors and data quality comprising remote function control, on-site check of
 212 sensors and cables, regular sensor calibration, data checks through different quality assurance
 213 procedures (e.g. exceedance of thresholds, outlier detection, deviations from other measurements),
 214 and data quality flagging.

215 3.1. Meteorology, soil temperature and soil moisture

216 All meteorological stations are located within the boundaries of the respective sites except for
 217 Klausen-Leopoldsdorf, where the station is at a distance of 2.7 km from the site. Meteorological
 218 measurements in the wetland sites were implemented next to the Eddy Covariance tower. In
 219 addition to the routine data checks, we compared the measurements with nearby stations where
 220 appropriate. Meteorological measurements were detected in a one-minute-interval and averaged
 221 over half-hour periods while rain data was summed. The measurements include air temperature,
 222 precipitation, relative humidity, wind speed and direction, air pressure, and several radiation
 223 variables (at least global radiation, but also short- and longwave radiation, photosynthetic active
 224 radiation, etc.).

225 *Table 2. Meteorological parameters measured at the six sites during 2019-2021. Availability is indicated using grey boxes.*
 226 *For parameter names we refer to the thesaurus at <http://vocabs.lter-europe.net/EnvThes/>*

227

Meteorological parameters

	KAS	KLL	NSS	PUE	ROS	ZOE
air relative humidity						
air pressure						
air temperature						
precipitation amount						
global radiation irradiance						
net radiation irradiance						
photosynthetically active radiation						
sunshine duration						
wind direction						
wind speed						

228

229 We used different types of soil temperature and soil moisture or soil water potential sensors,
 230 respectively (PT100 or thermoelements for soil temperature, TDR or FDR-sensors for soil moisture, and
 231 soil water potential sensors). Before we buried the soil temperature or soil moisture and soil water
 232 potential sensors into the soil, they had been calibrated or at least tested for consistency. Mostly, we
 233 used gravimetric samples to calibrate the TDR and FDR soil moisture sensors. At Zöbelboden, where
 234 stony, organic rich soils occur, we corrected the TDR values using water potential sensor data installed
 235 in the same soil profiles together with soil water retention functions derived from undisturbed soil
 236 cores. In addition to the regular QC procedures, we checked the data for consistency of the values
 237 across sensors (e.g. along the soil profiles) and compared them with other measurements (air
 238 temperature and precipitation). Half-hourly to hourly values are presented.

239 3.2. Carbon fluxes

240 3.2.1. Soil CO₂ efflux

241 We measured soil CO₂ efflux at five of the seven observation plots. The automated soil CO₂ respiration
 242 measurement systems are capable of operating autonomously during the snow-free periods. The
 243 measurement chambers and measurement systems collected air from the chamber headspace
 244 continuously to determine the exchange of CO₂ between soil and atmosphere at the observation plots.
 245 In all sites, we used non-steady state, non through-flow chambers (Pumpanen et al., 2004). The
 246 chambers at each site measured consecutively every half-hour to hour. In addition to the automated
 247 systems, manual flux measurements were also performed which served to validate the automated
 248 measurement systems. Table 3 provides detailed information on the measurement systems used at
 249 the sites.

250 Two different automated chamber systems were used: a LI-COR System and custom-made chambers
 251 in combination with LI-COR trace gas analysers (Table 3). The custom-made soil chambers are
 252 equipped with a fan and a thermometer. The controlling unit and the gas analyzer (either a CH₄/CO₂
 253 LI-COR 7810, a LI-COR 840, or a LI-COR 8100A, LI-COR Biosciences, USA) are located in already
 254 existing measurement containers. Remote access to the devices allows for checking plausibility of the
 255 data and chamber leakage in real time. We visited the instruments at weekly to monthly intervals,
 256 with maintenance and supervision works including a check of the tightness of the gas lines,
 257 connections and chamber lids, the correct closing and opening of the chambers and the functioning
 258 of ventilation fans inside the chambers, ingrowth of plants, and the gas analyser. The gas analysers
 259 were calibrated once a year in the laboratory with calibration gases. We de-installed and serviced the
 260 chambers during winter but frames stayed permanently on site to avoid disturbance of the soil.

261 At Klausen-Leopoldsdorf, the gas fluxes of readings were determined using the R package "gasfluxes"
 262 (Fuss, 2020). At Rosalia, a custom-made Python script was used. Zöbelboden and Kaserstattalm
 263 process the data with SoilFlux Pro Software (LI-COR Biosciences, 2019). We used the R² of the fitted
 264 empirical models to select valid data. We refer to Table 3 and the metadata published with the data
 265 for the detailed specifications.

266 *Table 3. Specifications of the different soil CO₂ flux systems following the standard of (Bond-Lamberty et al., 2021).*

Field Name	Description	Unit	Klausen- Leopoldsdorf	Stubai grassland	Rosalia	Zöbelboden
System			auto	Auto	auto	auto

GHG chambers			Custom-made (n=12)	LI-8100-104 (n=4)	Custom-made (n=12)	LI-8100-104 (n=6)
INSTRUMENT	Measurement instrument model		LI-COR LI-7810	LI-8100A	LI-840	LI-8100A
MSMT_VAR	Type of flux measured		Soil respiration (Rs)			
AREA	Soil surface measurement area	cm ²	2500	317.8	2500	317.8
VOLUME	Volume of measurement chamber	cm ³	37500	4076.1	37500	4076.1
V/A	Volume/Area ratio	cm	15	12.83	15	12.83
COLLAR_DEPTH	Depth of collar insertion	cm	5	2	10	2
OPAQUE	Opaque chamber		no	Yes	no	yes
chamber system	static chamber - closed or open		non-steady state, non through-flow chambers			
closing time	closing time of chamber (=time used for flux calculation)	sec	175	depending on year	1620	210
PLANTS_REMOVED	Plants removed from inside the collar		no, but hardly any	Yes	no, but hardly any	no plants
flow_rate	sample flow rate through tubing	l min ⁻¹	1	1 to 2	0.25	1.7
FAN	Mixing fan in chamber?		yes	No	yes	no
CRVFIT_CO2	Flux computation method ("Lin" or "Exp" for linear and exponential, others)		linear	automated ¹	Lin/HMR ²	Automated ¹
R2_CO2	R ² of flux computation	fraction	0.90	0.95	0.95	0.99
Calculation of flux			R Package gasfluxes	LI-COR Soilflux Pro	custom-made python script	LI-COR Soilflux Pro

¹ "Exp" in the data indicates that the exponential fit was better than the linear fit (Exp_SSN < Lin_SSN). "Lin" indicates that the linear fit was better after the maximum number of iterations; the non-linear coefficients have therefore been derived from the linear fit.

² Hutchinson and Mosier (1981)

268 In both wetland sites, the Pürgschachen Moor and Lake Neusiedl, fully equipped Eddy-Covariance
 269 systems are in place. Wind speed and direction were measured using a three-axis ultrasonic
 270 anemometer (WindMaster Pro, Gill Instruments, Lymington, UK). CO₂ and H₂O mixing ratios were
 271 measured using the closed-path infrared gas analyser LI-7200 while CH₄ was detected with the open
 272 path gas analyser LI-7700 (both LI-COR Inc, Lincoln, USA). The measurements were performed with a
 273 sampling rate of 10 Hz. We installed the devices at a vegetation dependent height, 3.05 m above
 274 ground in the Pürgschachen Moor and in the reed belt of Lake Neusiedl 8.6 m, respectively. The Eddy
 275 Covariance devices were checked daily via remote access, calibrated once a year in the lab, and
 276 monthly in the field.

277 The EC data contains half-hour eddy covariance flux measurements for CO₂, CH₄ and water vapor. We
 278 calculated the fluxes with the EddyPro® Software package in the Express mode with default settings
 279 (double rotation, block averaging, covariance maximization, etc.) as part of the SmartFlux® 2 System,
 280 providing fully corrected and valid fluxes with quality flags ranging from 0-2. The final flags are based
 281 on a combination of partial flags accounting for steady state and turbulent conditions. Only fluxes
 282 flagged with 0 (best quality fluxes) or 1 (fluxes suitable for general analysis such as annual budgets)
 283 are shown in the data. Gaps in the data-set result from missing micro-meteorological conditions,
 284 from data cleaning due to the quality flags or from power breakdowns.

285 3.3. Radial tree stem growth at forest sites

286 Zöbelboden, Klausen-Leopoldsdorf, Rosalia used the DR26 sensor (EMS, Brno, Czech Republic), Stubai
 287 used Ecomatic DC2 (Germany) for registering the radial stem increment in a 15 minutes to 30 minutes
 288 interval. Maintenance involved avoiding any shift of the sensor during the operation. Concerning data
 289 quality and control methods the Mini32 software (EMS, Brno, Czech Republic), includes graphical
 290 features to process the measured stem increment data. Data processing comprises outlier detection
 291 by visual assessment based on expert knowledge. Ecomatic raw data was treated with custom-made
 292 R scripts. In both cases, unrealistic values beyond the slowly increasing linear growth rates were
 293 visually assessed and deleted.

294 4. Data file structure

295 We used the eLTER Data specification, which is available on Zenodo
 296 (www.doi.org/10.5281/zenodo.6373409). Apart from the data files, the measurement locations
 297 (Station files) and the sensors (methods) are included.

298

299 5. Data validation

300 *Table 4. Comparison between long-term (1980-2010) meteorological drought (SPEI - Standardized Precipitation*
 301 *Evapotranspiration Index) and the measurement years during the growing season (May-September). Significant differences*
 302 *between these years and the long-term averages are shown: *** p<0.001; ** p<0.005; * p<0.01 according to a Mann-*
 303 *Whitney U Test. SPEI was calculated using a 30 days window in a daily resolution using gridded data:*
 304 *<https://data.hub.geosphere.at/dataset/winfore-v2-1d-1km> (Haslinger & Bartsch, 2016). Negative values indicate dry years.*

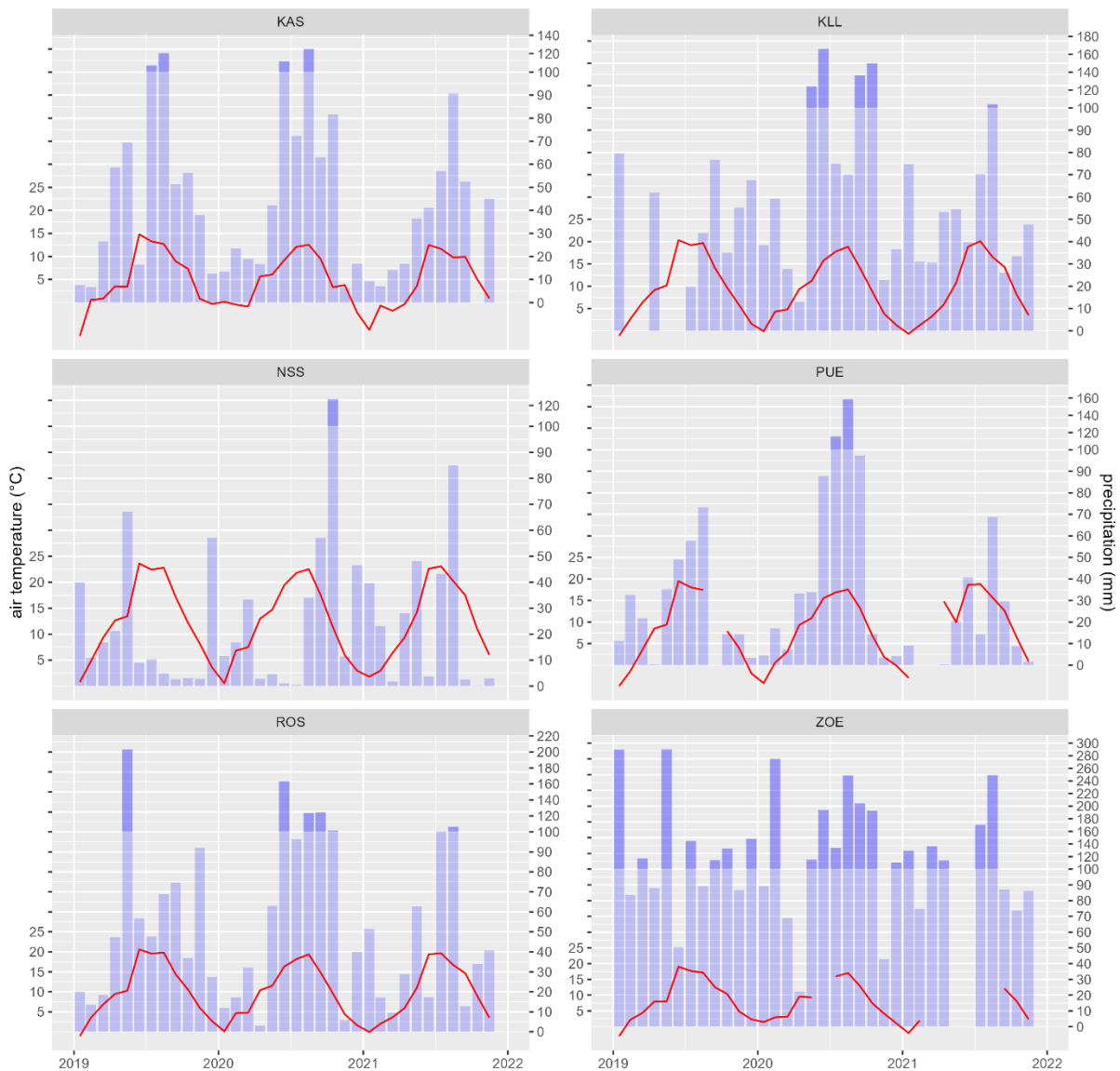
Site Code	1980-2010	2019	2020	2021
ZOE	-0.05±0.94	-0.49±1.22***	0.42±0.69***	-0.02±1.39
KLL	-0.01±0.99	-0.23±1.22	0.39±0.86***	-0.02±1.24
KAS	-0.05±0.97	-0.1±1.17	-0.12±0.78	0.23±1.07**
PUE	-0.02±0.94	-0.54±1.26***	0.17±0.59**	-0.12±1.2
NSS	-0.01±1	-0.22±1.13*	0.2±0.87**	-0.2±1.34
ROS	-0.03±0.98	-0.34±1.01***	0.17±0.83	-0.28±1.08

305

306 We used gridded SPEI (Standardized Precipitation Evapotranspiration Index) from the Austrian
307 Meteorological Service (<https://data.hub.geosphere.at/dataset/winfore-v2-1d-1km>; Haslinger &
308 Bartsch (2016)) to compare the long-term average water availability during the growing season
309 (1980-2010; May to September) with those occurring in the measurement years (Table 4). The
310 advantage of the SPEI is that it accounts for precipitation and temperature via evapotranspiration
311 and integrates over a given temporal window (we used 30 days) (Vicente-Serrano et al. 2010).
312 Accordingly, the 2021 was closest to the long-term average, the year 2020 was a particularly wet
313 year, and the year 2019 was drier than the average. However, there were differences between the
314 sites: particularly the mountain station in the Tyrolian Alps (KAS) did not experience significant
315 deviations in SPEI as compared to the long-term average apart from a wet growing season in 2021.
316 The SPEI at the site in the Viennese Forest (KLL) does not indicate that in 2019, the growth period
317 was particularly dry.

318 The monthly precipitation and temperature patterns are shown in Figure 2, and soil water content
319 and soil temperatures in Figure 3 and Figure 5. Differences in the seasonal precipitation patterns
320 between the measurement years vary a lot between sites. In sum, lower precipitation occurred in
321 2019 and 2021 than in 2020 in all sites. The mean annual temperature maxima (90 percentile) were
322 between 0.3 °C (KAS) and 2.3 °C (ZOE) higher in the year 2019 than in 2020. These differences were
323 lower when comparing the year 2021 with 2019 (≤ 0.6 °C). In accordance with SPEI, precipitation and
324 temperature, soil water content showed the lowest values during the years 2019 followed by the
325 year 2021, and soil temperature were higher during these years (Figure 3Figure 4).

326



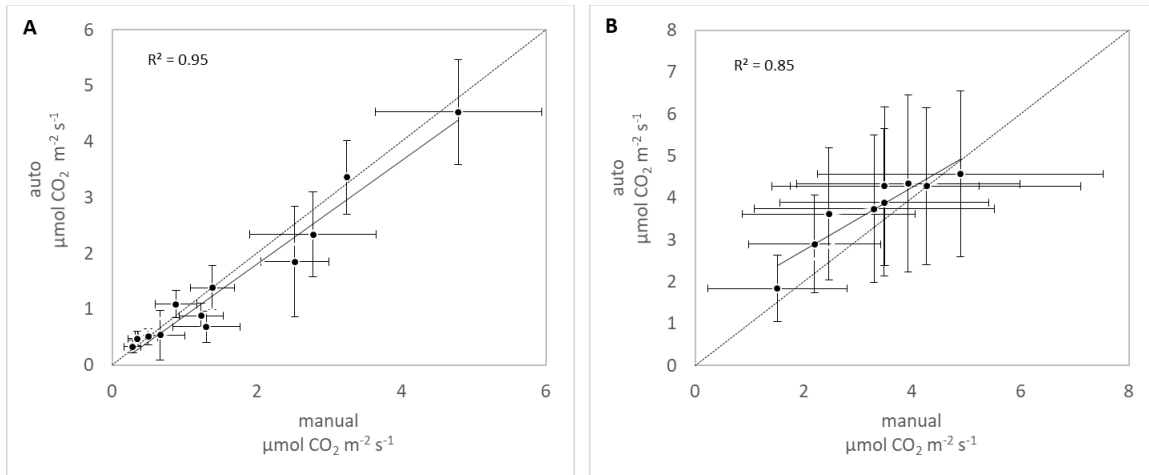
327

328 *Figure 2. Monthly mean air temperature (red line) and monthly precipitation sums (blue bars; different scale > 100 mm) at*
 329 *the six regions.*

330 We measured soil CO₂ respiration at four sites (Figure 4). The complexity of automated chamber
 331 measurements resulted in some data gaps: at KAS and ROS during the years 2019 and 2021
 332 respectively; at KLL and ZOE, the respiration data covers most of the snow-free period (see Table 2).

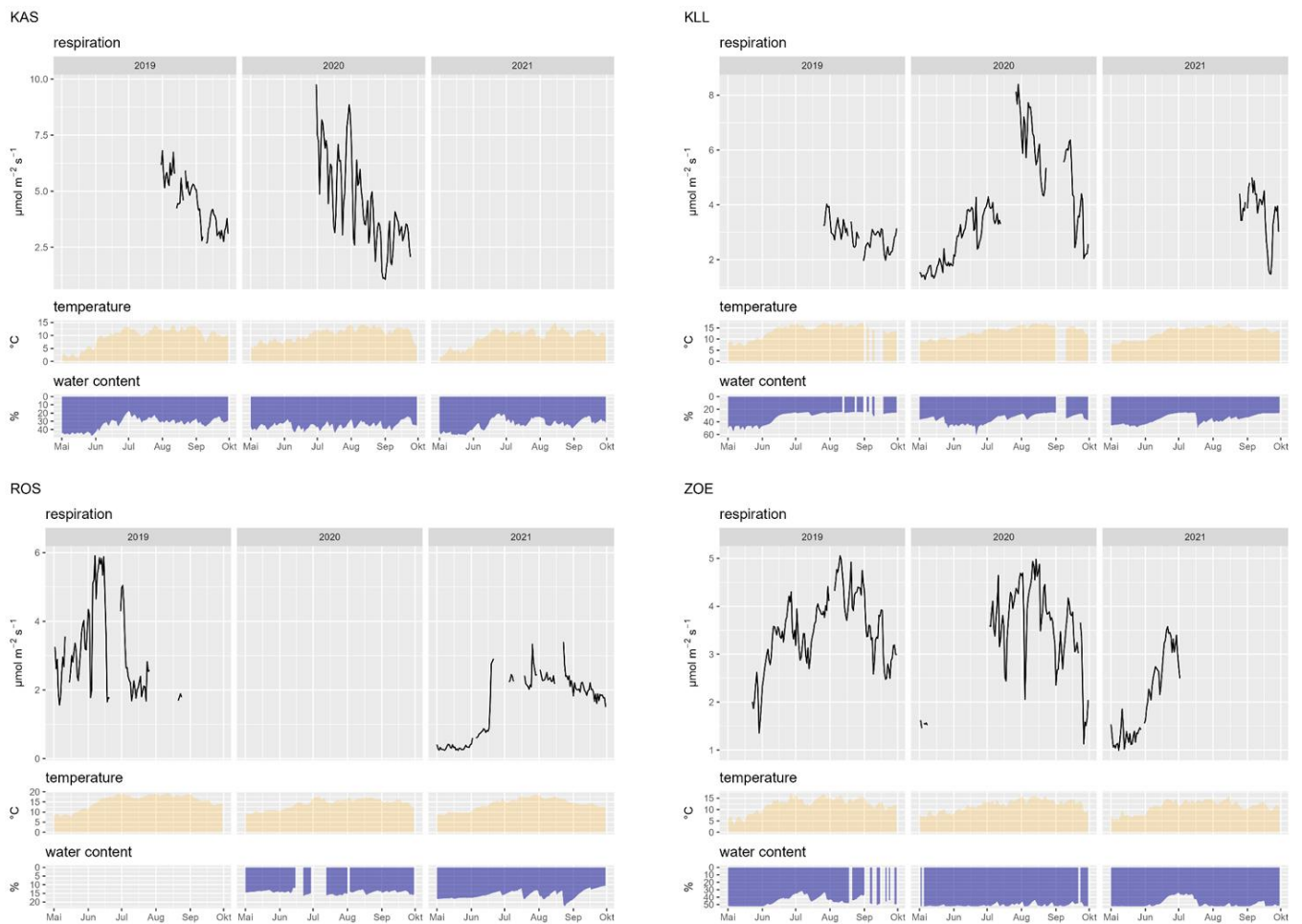
333 At Klausen-Leopoldsdorf (KLL) and Zöbelboden (ZOE), we compared the automatically measured soil
 334 CO₂ flux rates with manual measurements. For both sites, we used a portable infrared gas analyzer
 335 (EGM-4) connected to a manual soil respiration chamber (SRC) (PP Systems International Inc.,
 336 Amesbury, MA, USA). The two measurement sites were equipped with permanently installed collars
 337 (KLL: randomly distributed within the site in immediate vicinity of the automated chambers (n = 12);
 338 area = 284 cm² and 2 cm insertion depth; Zöbelboden: regular grid covering the entire plot (n = 30),
 339 area = 78 cm² and 1.5 cm insertion depth). The chamber closure time was 60 and 100 seconds in KLL
 340 and ZOE, respectively. Manual measurements took place in monthly intervals from Oct. 2019-Jun.
 341 2020 at Klausen-Leopoldsdorf and from Jun. 2019 until Oct. 2019 (monthly interval) and in July 2020
 342 (diurnal variation) at ZOE. Soil respiration (Rs) was calculated automatically by fitting a linear (KLL) or
 343 quadratic function (ZOE; quadratic fit for flow rates > 0.2 ppm s⁻¹, otherwise a linear fit was used) to
 344 the increasing CO₂ headspace concentration.

345 The mean CO₂ fluxes of the automated chambers correlated well with the manually measured fluxes
 346 during the measurement campaigns (Figure 3). At KLL, the R² was 0.95 (p-value < 0.05, t-test), at ZOE
 347 it was 0.85 (p-value < 0.05, t-test). In both sites, neither the intercept nor the slope was significantly
 348 different from 0 (p-value > 0.2, t-test) and 1 (p-value > 0.49, t-test), respectively. At ZOE, the spatial
 349 flux variation was much higher than at KLL (Figure 3A and 3B). This reflects the heterogeneity of the
 350 soil conditions (shallow rendzic leptosols with interspersed fine-scale patches of deeper soils), the
 351 canopy gaps (with lower root density), and the uneven distribution of litter due to the steep slope at
 352 the plot, more effectively captured in the manual measurement (n=30) than by the automated
 353 chambers (n=6). In summary, we conclude that the spatial variation in CO₂ fluxes was higher at both
 354 sites than the difference in fluxes caused by the measurement devices (Figure 3).



355
 356 *Figure 3.* Comparison of automated and manual soil CO₂ fluxes at A) Klausen-Leopoldsdorf and B) Zöbelboden. See *Table 3*
 357 for the specification of automated chamber data. Error bars indicate spatial variation (standard deviations).

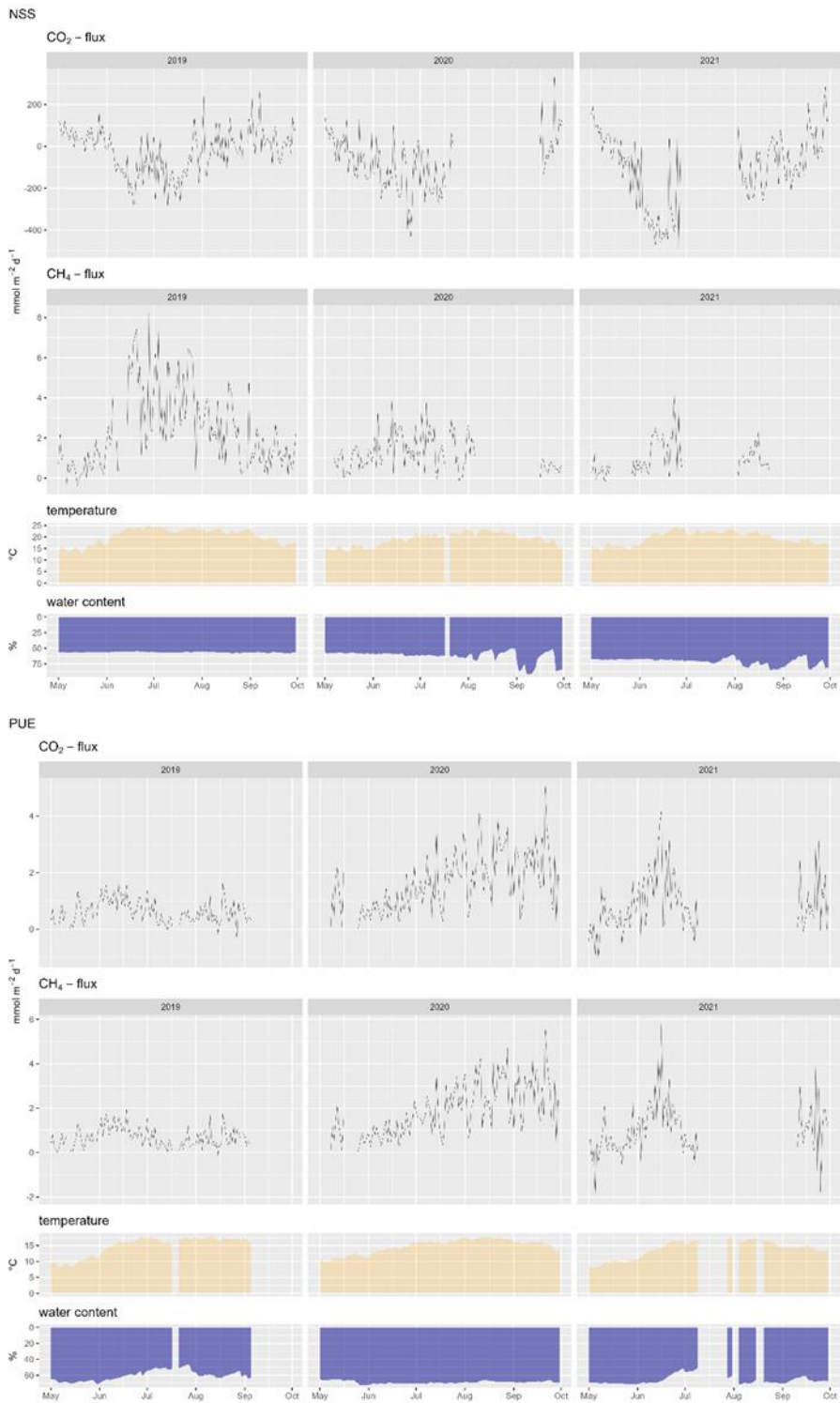
358



359

360 *Figure 4. Soil CO₂ respiration (mean of all chambers), soil temperature (mean of sensors in 5-15 cm depth) and soil water*
 361 *content (mean of sensors in 5-15 cm depth) in the forested sites Kaserstattalm forest (KAS), Klausen-Leopoldsdorf (KLL),*
 362 *Rosalia (ROS), and Zöbelboden (ZOE).*

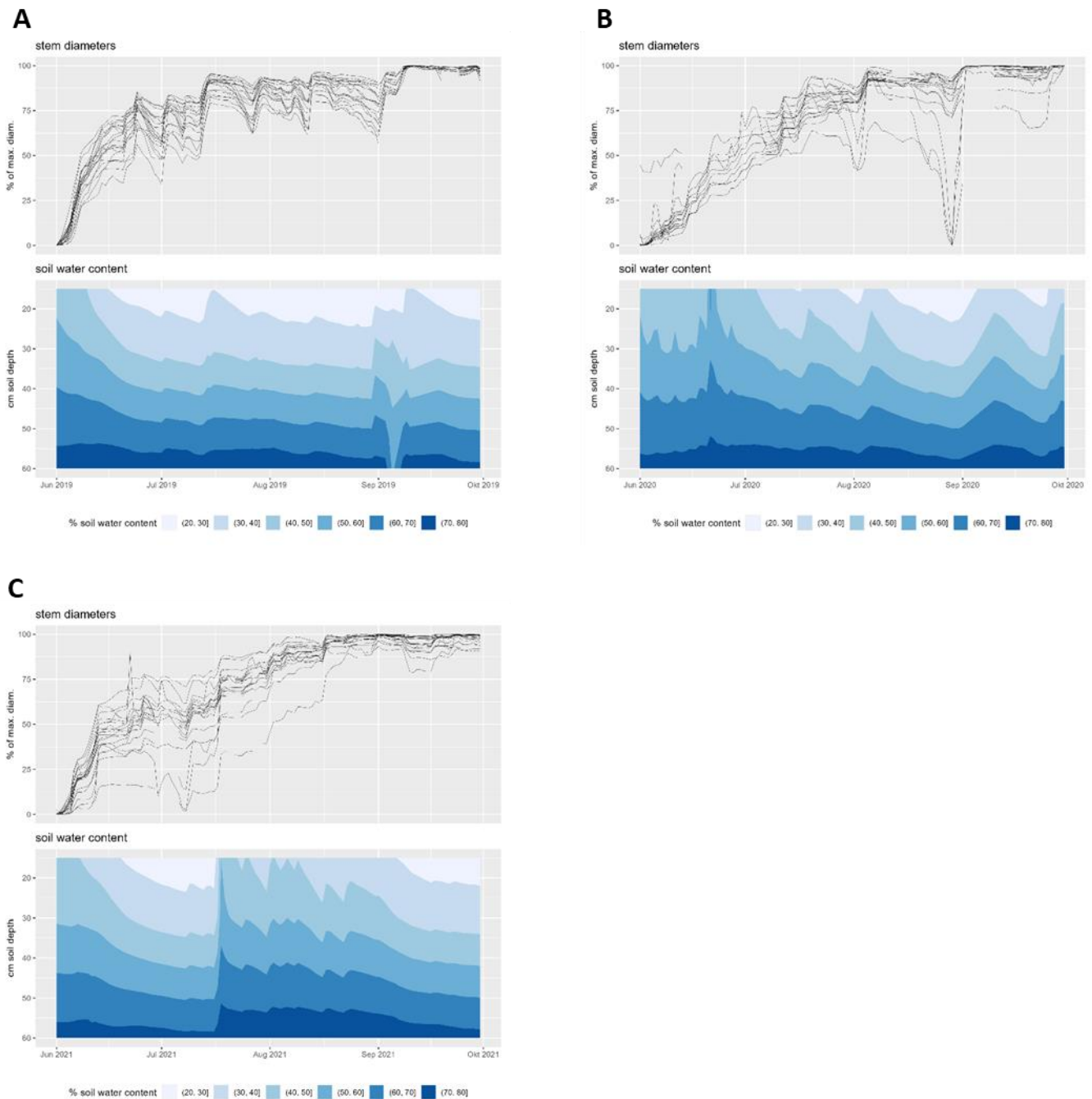
363 Soil CO₂ fluxes are temperature dependent, thus follow the seasonal changes in soil temperature
 364 (Figure 4). Their additional limitation through soil water availability for plant metabolism and
 365 microbial activity is usually much less pronounced in these temperate zone ecosystems (Bahn et al.
 366 2008; Chen et al. 2014). For detailed interpretation of the CO₂ respiration fluxes and their limiting
 367 factors, we refer to the citations listed in the site description chapter. Drollinger et al. (2019)
 368 provides interpretations of the patterns of CO₂ and CH₄ fluxes, measured using Eddy covariance
 369 techniques at the bog site Pürgschachen Moor (PUE), and likewise, Baur et al. (2024), for the reed
 370 belt of Neusiedler See (NSS). Stem growth limitations can, on the other hand, be closely related to
 371 soil water content, particularly at sites with relatively low precipitation such as Klausen-Leopoldsdorf
 372 (KLL) (Figure 6). For an in-depth study of drought related effects on tree growth at the treeline forest
 373 at Kasterstattalm (KAS), we refer to Oberleitner et al. (2022).



374

375 *Figure 5. CO₂ and CH₄ fluxes in the sites Lake Neusiedl reed zone (NLL) and Pürgschachen Moor peat bog (PUE) as well as soil*
 376 *water content and temperature*

377



378

379 *Figure 6. Relative stem diameters and soil moisture at the site Klausen-Leopoldsdorf (KLL) during the dry years 2019 (A),*
 380 *2020 (B), and 2021 (C). Stem diameter values were scaled to an annual amplitude of 100.*

381

382 6. Discussion

383 We provide baseline ecosystem data related to the carbon cycle and capture naturally occurring ECEs
 384 across various ecosystem types typical for Austria and other regions of Central Europe. Such data sets
 385 are scarce because the measurements are demanding in terms of maintenance and funding.
 386 Automated soil respiration data in high temporal resolution, as we report it here, is rare too owing to
 387 a lack of dedicated monitoring or research infrastructures (Bond-Lamberty et al., 2021). However,
 388 soil CO₂ respiration constitutes the second-largest flux in the global carbon cycle, hence is key in
 389 estimating ecosystem response to ECEs (Bond-Lamberty and Thomson, 2010). In addition, we

390 provide soil temperature and moisture measurements in the same resolution, being key variables
391 determining soil respiration (Pumpanen et al., 2015). High-resolution measurements of tree stem
392 circumference have been developed as complementary data to relate drought stress with changes in
393 carbon allocation in trees (Zweifel, 2016; Zweifel et al., 2021). The microclimatic, soil, and tree
394 physiological data is complemented by CO₂ and CH₄ fluxes between the vegetation and the
395 atmosphere measured with Eddy covariance techniques of the two wetland sites.

396 Our data is particularly useful for drought-related research. Triggered by the pan-European drought
397 of 2003 (Ciais et al., 2005), a key scientific question has been how droughts affect greenhouse gas
398 sinks and sources in ecosystems (Rödenbeck et al., 2020; Reichstein et al., 2013; Anderegg et al.,
399 2020). Droughts usually reduce soil respiration due to the decrease in autotrophic respiration but
400 also because soil microbial activity drops due to water limitation (Grünzweig et al., 2022).
401 Furthermore, rewetting can result in pulses of high soil respiration (Borken and Matzner, 2009).
402 Drought effects on the ecosystem C cycle can persist for years (Kannenbergh et al., 2020; Müller and
403 Bahn, 2022) and novel approaches are being developed for assimilating high-resolution data for
404 understanding and quantifying such legacies (Yu et al., 2022; Fu et al., 2020). In this context, the
405 availability of long-term, high-resolution measurements of key ecosystem parameters is key for
406 understanding and quantifying the effects of recurrent droughts (Oberleitner et al., 2022). While the
407 three-year data with the usual measurement gaps occurring in field campaigns in rather difficult
408 terrain can only to some extent capture aspects of drought related effects, it represents a valuable
409 baseline.

410

411 The sites presented here are currently being upgraded towards their implementation in the
412 European Research Infrastructure for Integrated European Long-Term Ecosystem, critical zone and
413 socio-ecological Research (eLTER RI), together with another ~200 sites in Europe (Mirtl et al., 2018).
414 Climate change impacts on ecosystem processes including the carbon cycle are among the targeted
415 research areas the eLTER RI will focus on. The measurements resulting in the data presented here
416 will continue in future under the umbrella of eLTER RI. Compiling longer-term data series depends
417 upon the availability of already validated data sets - as it is presented here - before the RI is being
418 operational. Furthermore, long-term ecosystem observations already exist in these sites with regard
419 to water and nitrogen cycle allowing for a contextual interpretation of the trends seen in C related
420 parameters.

421 Combining several research and monitoring activities at already heavily instrumented sites not only
422 saves money but widens the data analyses portfolio (Futter et al. 2023; Kulmala 2018). Even though
423 we provide Eddy covariance data for two of our sites, Austria is not part of the Integrated Carbon
424 Observation System (ICOS). A combination of data capturing long-term boundary layer exchange of C
425 together with soil C fluxes, microclimate, and, in forests, tree physiological data obviously holds great
426 potential (Zweifel et al., 2023; Ramonet et al., 2020). Hence, using the sites simultaneously for other
427 research infrastructures, such as ICOS, providing high-quality Eddy covariance measurements would
428 obviously be ideal. The more so because European Research Infrastructures follow the FAIR data
429 principles to make data Findable, Accessible, Interoperable and Reusable (Wilkinson et al., 2016).

430 While the eLTER RI data infrastructure is still under development, we comply with the standards
431 already implemented. We used DEIMS-SDR (<https://deims.org/>) as the catalogue documenting the
432 sites (Wohner et al., 2019; Wohnner et al., 2022). It issues persistent identifiers for sites (see Table 1)
433 that allow to uniquely identify sites across research projects and networks. Tools are being
434 developed to query available information about sites programmatically (Oggioni et al., 2023;
435 Wohnner, 2023) providing contextual ecosystem information.

436

437 7. Data availability

438 7.1 Data access

439 The data and metadata is accessible at B2SHARE (<https://b2share.eudat.eu/>), a service provided by
 440 the EUDAT Collaborative Data Infrastructure. DOIs of the datasets are listed in Table 5. The site
 441 metadata in DEIMS-SDR (Table 1) is part of the data metadata so that site information can easily be
 442 accessed. In chapter8, we provide a jupyter notebook to download and merge the single datasets,
 443 and to visualize parameters.

444 *Table 5. Dataset DOIs*

Site	Dataset	DOI	Reference
Klausen- Leopoldsdorf	Meteorology	https://doi.org/10.23728/b2share.8f872a37513c4768b16ce755eca4bb57	(Gartner et al., 2024a)
	Soil climate	https://doi.org/10.23728/b2share.8d49c0b557f1455a9e66689e035b8cce	(Gartner et al., 2024b)
	Soil CO ₂ respiration	https://doi.org/10.23728/b2share.5286bd1bc6aa491f874b9bb12d1c5673	(Kitzler and Hofbauer, 2024)
	Stem increment	https://doi.org/10.23728/b2share.68d84a913f0c4875be5c680ad4d6959e	(Gartner and Gollobich, 2024)
Rosalia Forest Demonstration Centre	Meteorology	https://doi.org/10.23728/b2share.96c52c247eb846deb2a3ec5e2c27b4f1	(Diaz-Pines, 2024a)
	Soil climate	https://doi.org/10.23728/b2share.c68143fc11224c44ae5529bd6a35a76d	(Diaz-Pines, 2024c)
	Soil CO ₂ respiration	https://doi.org/10.23728/b2share.d167e727abe947abbc8efc04057557f6	(Diaz-Pines, 2024b)
	Stem increment	https://doi.org/10.23728/b2share.d0d185f1eb184ae48f6d06ea9aa8dbdf	(Diaz-Pines, 2024d)
Zöbelboden	Meteorology	https://doi.org/10.23728/b2share.762e665273234b129d09ef017416bcfb	(Kobler et al., 2024a)
	Soil climate	https://doi.org/10.23728/b2share.46e19191ce9c427d90f48ce38f56a0e1	(Kobler et al., 2024c)
	Soil CO ₂ respiration	https://doi.org/10.23728/b2share.4f44006b932142e68981106a016f1f56	(Kobler et al., 2024b)
	Stem increment	https://doi.org/10.23728/b2share.2de5b37a0cad4f82a19f477531d6af24	(Pröll et al., 2024)
Stubai - Kaserstattalm	Meteorology	https://doi.org/10.23728/b2share.77462914dc0b43cb8c24a967e6851665	(Ingrisch and Bahn, 2024c)
	Soil climate	https://doi.org/10.23728/b2share.026d76094e8f4512b09b35b7a0d2a9d7	(Ingrisch and Bahn, 2024d)
	Soil CO ₂ respiration	https://doi.org/10.23728/b2share.cfe8c7ad1965433484650ea9026512ca	(Ingrisch and Bahn, 2024a)
	Stem increment	https://doi.org/10.23728/b2share.0e3eed54ff30418f8720806b5f05cca9	(Ingrisch and Bahn, 2024b)
Pürgschachen Moor	Meteorology	https://doi.org/10.23728/b2share.5442510ad03e4968afb4e2108e85a64d	(Maier and Glatzel, 2024e)
	Soil climate	https://doi.org/10.23728/b2share.9380364098d14978b876a87517652d62	(Maier and Glatzel, 2024f)
	Eddy Covariance	https://doi.org/10.23728/b2share.4f783e3ff2884abca5c59960db0b7955	(Maier and Glatzel, 2024d)

	Meteorology	https://doi.org/10.23728/b2share.f7176c9ee982464f947d2fe9fb8f389d	(Maier and Glatzel, 2024b)
Lake Neusiedl	Soil climate	https://doi.org/10.23728/b2share.4e6474cd55f9487d97e3d31e83baa530	(Maier and Glatzel, 2024c)
	Eddy Covariance	https://doi.org/10.23728/b2share.b83caca3efe44868a1ed49129b4a576a	(Maier and Glatzel, 2024a)

445

446 7.2 Data visualization, workflow integration

447 The software stack used to store, import and quality control the provided data is built on PostgreSQL
 448 database with a Post-GIS extension. The database structure is derived from the Time Series
 449 Management (TSM) system developed by the Research Center Jülich (Wohner, C., Dirnböck, T.,
 450 Peterseil, J., Pröll, G., Geiger, S., 2021) and originally deployed during the LTER CWN project but was
 451 repurposed to better fit the needs of the data management and working group. Now, for the import
 452 and quality control of data, a number of Python scripts deployed in a Jupyter environment are used.
 453 This is also includes scripts to visualise the data on the fly in Jupyter.

454

455 8. Code availability

456 A Jupyter notebook to access, merge, and visualize the data from all sites is available at
 457 <https://gist.github.com/10/9bbe44a03f12801c6c742202b005db57>.

458

459 9. Author contribution

460 DT, BM, DPM, DI, EM, GK, GG, MA, IJ, KB, KJ, MA, PG, VS, ZBS, ZA, and GS designed the
 461 measurements and carried them out. WC, PJ designed and constructed the database. KK, VS, and PG
 462 customized and filled the database. OI developed the Jupyter notebook. DT prepared the manuscript
 463 with contributions from all co-authors.

464

465 10. Competing interests

466 The authors declare that they have no conflict of interest.

467

468 11. Acknowledgements

469 We want to thank Manfred Bogner, Thomas Lehner, Christian Holtermann, Thomas Kager, and Josef
 470 Gasch for technical implementation and assistance.

471

472 12. Funding

473 The infrastructure and its implementation was funded by the Austrian Research Promotion Agency
 474 (FFG, project LTER-CWN: Long-Term Ecosystem Research Infrastructure for Carbon, Water and
 475 Nitrogen, grant no. 858024). The Austrian Academy of Sciences (ÖAW) supported all authors for data
 476 compilation and writing of the manuscript through its eLTER 2022 call (Earth System Sciences (ESS)).
 477 T.D., J.K., K.K., J.P., C.W. and E.D-P. received additional funding from the EU Horizon 2020 project

478 eLTER PLUS (grant no. 871128), and E.D-P. also from the project EXAFOR (Austrian Climate Research
479 Programme 12th Call, grant no. KR19AC0K17557).

480

481 13. References

- 482 Anderegg, W. R. L., Trugman, A. T., Badgley, G., Anderson, C. M., Bartuska, A., Ciais, P., Cullenward,
483 D., Field, C. B., Freeman, J., Goetz, S. J., Hicke, J. A., Huntzinger, D., Jackson, R. B., Nickerson, J.,
484 Pacala, S., and Randerson, J. T.: Climate-driven risks to the climate mitigation potential of forests,
485 *Science*, 368, eaaz7005, <https://doi.org/10.1126/science.aaz7005>, 2020.
- 486 Baatz, R., Hendricks Franssen, H. J., Euskirchen, E., Sihi, D., Dietze, M., Ciavatta, S., Fennel, K., Beck,
487 H., Lannoy, G. de, Pauwels, V. R. N., Raiho, A., Montzka, C., Williams, M., Mishra, U., Poppe, C.,
488 Zacharias, S., Lausch, A., Samaniego, L., van Looy, K., Bogena, H., Adamescu, M., Mirtl, M., Fox, A.,
489 Goergen, K., Naz, B. S., Zeng, Y., and Vereecken, H.: Reanalysis in Earth System Science: Toward
490 Terrestrial Ecosystem Reanalysis, *Reviews of Geophysics*, 59,
491 <https://doi.org/10.1029/2020RG000715>, 2021.
- 492 Bahn, M. and Ingrisch, J.: Accounting for Complexity in Resilience Comparisons: A Reply to Yeung and
493 Richardson, and Further Considerations, *Trends in Ecology & Evolution*, 33, 649–651,
494 <https://doi.org/10.1016/j.tree.2018.06.006>, 2018.
- 495 Bahn, M., Rodeghiero, M., Anderson-Dunn, M., Dore, S., Gimeno, C., Drösler, M., Williams, M.,
496 Ammann, C., Berninger, F., Flechard, C., Jones, S., Balzarolo, M., Kumar, S., Newesely, C.,
497 Priwitzer, T., Raschi, A., Siegwolf, R., Susiluoto, S., Tenhunen, J., Wohlfahrt, G., and Cernusca, A.:
498 Soil Respiration in European Grasslands in Relation to Climate and Assimilate Supply, *Ecosystems*,
499 11, 1352–1367, <https://doi.org/10.1007/s10021-008-9198-0>, 2008.
- 500 Bahn, M., Schmitt, M., Siegwolf, R., Richter, A., and Brüggemann, N.: Does photosynthesis affect
501 grassland soil-respired CO₂ and its carbon isotope composition on a diurnal timescale?, *New*
502 *Phytologist*, 182, 451–460, <https://doi.org/10.1111/j.1469-8137.2008.02755.x>, 2009.
- 503 Baur, P. A., Henry Pinilla, D., and Glatzel, S.: Is ebullition or diffusion more important as methane
504 emission pathway in a shallow subsaline lake?, *Science of The Total Environment*, 912, 169112,
505 <https://doi.org/10.1016/j.scitotenv.2023.169112>, 2024.
- 506 Bernal, S., Hedin, L. O., Likens, G. E., Gerber, S., and Buso, D. C.: Complex response of the forest
507 nitrogen cycle to climate change, *Proceedings of the National Academy of Sciences*, 109, 3406–
508 3411, <https://doi.org/10.1073/pnas.1121448109>, 2012.
- 509 Bond-Lamberty, B. and Thomson, A.: Temperature-associated increases in the global soil respiration
510 record, *Nature*, 464, 579–582, 2010.
- 511 Bond-Lamberty, B., Christianson, D. S., Crystal-Ornelas, R., Mathes, K., and Pennington, S. C.: A
512 reporting format for field measurements of soil respiration, *Ecological Informatics*, 62, 101280,
513 <https://doi.org/10.1016/j.ecoinf.2021.101280>, 2021.
- 514 Borken, W. and Matzner, E.: Reappraisal of drying and wetting effects on C and N mineralization and
515 fluxes in soil, *Global Change Biology*, 15, 808–824, 2009.
- 516 Buchsteiner, C., Baur, P. A., and Glatzel, S.: Spatial Analysis of Intra-Annual Reed Ecosystem Dynamics
517 at Lake Neusiedl Using RGB Drone Imagery and Deep Learning, *Remote Sensing*, 15, 3961,
518 <https://doi.org/10.3390/rs15163961>, 2023.
- 519 Chen, S., Zou, J., Hu, Z., Chen, H., and Lu, Y.: Global annual soil respiration in relation to climate, soil
520 properties and vegetation characteristics: Summary of available data, *Agricultural and Forest*
521 *Meteorology*, 198-199, 335–346, <https://doi.org/10.1016/j.agrformet.2014.08.020>, 2014.
- 522 Ciais, P., Reichstein, M., Viovy, N., Granier, A., Ogée, J., Allard, V., Aubinet, M., Buchmann, N.,
523 Bernhofer, C., Carrara, A., Chevallier, F., Noblet, N. de, Friend, A. D., Friedlingstein, P., Grünwald,
524 T., Heinesch, B., Keronen, P., A. Knohl, A., Krinner, G., Loustau, D., Manca, G., Matteucci, G.,

525 Miglietta, F., Ourcival, J. M., Papale, D., Pilegaard, K., Rambal, S., Seufert, G., Soussana, J. F., M. J.
526 Sanz, Schulze, E.-D., Vesala, T., and Valentini, R.: Europe-wide reduction in primary productivity
527 caused by the heat and drought in 2003, *Nature*, 437, 529–533, 2005.

528 Diaz-Pines, E.: Rosalia forest (Austria) - meteorological data (2020-2021),
529 <https://doi.org/10.23728/B2SHARE.96C52C247EB846DEB2A3EC5E2C27B4F1>, 2024a.

530 Diaz-Pines, E.: Rosalia forest (Austria) - soil CO2 respiration (2019-2021),
531 <https://doi.org/10.23728/B2SHARE.D167E727ABE947ABBC8EFC04057557F6>, 2024b.

532 Diaz-Pines, E.: Rosalia forest (Austria) - soil temperature and soil moisture (2019-2021),
533 <https://doi.org/10.23728/B2SHARE.C68143FC11224C44AE5529BD6A35A76D>, 2024c.

534 Diaz-Pines, E.: Rosalia forest (Austria) - tree increments (2019-2021),
535 <https://doi.org/10.23728/B2SHARE.D0D185F1EB184AE48F6D06EA9AA8DBDF>, 2024d.

536 Dirnböck, T., Brielmann, H., Djukic, I., Geiger, S., Hartmann, A., Humer, F., Kobler, J., Kralik, M., Liu, Y.,
537 Mirtl, M., and Pröll, G.: Long- and Short-Term Inorganic Nitrogen Runoff from a Karst Catchment
538 in Austria, *Forests*, 11, 1112, <https://doi.org/10.3390/f11101112>, 2020.

539 Dirnböck, T., Haase, P., Mirtl, M., Pauw, J., and Templer, P. H.: Contemporary International Long-
540 Term Ecological Research (ILTER)—from biogeosciences to socio-ecology and biodiversity
541 research, *Reg Environ Change*, 19, 309–311, <https://doi.org/10.1007/s10113-018-1445-0>, 2019.

542 Dirnböck, T., Kobler, J., Kraus, D., Grote, R., and Kiese, R.: Impacts of management and climate
543 change on nitrate leaching in a forested karst area, *Journal of Environmental Management*, 165,
544 243–252, <https://doi.org/10.1016/j.jenvman.2015.09.039>, 2016.

545 Drollinger, S., Maier, A., and Glatzel, S.: Interannual and seasonal variability in carbon dioxide and
546 methane fluxes of a pine peat bog in the Eastern Alps, Austria, *Agricultural and Forest
547 Meteorology*, 275, 69–78, <https://doi.org/10.1016/j.agrformet.2019.05.015>, 2019.

548 Frank, D., Reichstein, M., Bahn, M., Thonicke, K., Frank, D., Mahecha, M. D., Smith, P., van der Velde,
549 M., Vicca, S., Babst, F., Beer, C., Buchmann, N., Canadell, J. G., Ciais, P., Cramer, W., Ibrom, A.,
550 Miglietta, F., Poulter, B., Rammig, A., Seneviratne, S. I., Walz, A., Wattenbach, M., Zavala, M. A.,
551 and Zscheischler, J.: Effects of climate extremes on the terrestrial carbon cycle: concepts,
552 processes and potential future impacts, *Global Change Biology*, 21, 2861–2880,
553 <https://doi.org/10.1111/gcb.12916>, 2015.

554 Fu, Z., Ciais, P., Bastos, A., Stoy, P. C., Yang, H., Green, J. K., Wang, B., Yu, K., Huang, Y., Knohl, A.,
555 Šigut, L., Gharun, M., Cuntz, M., Arriga, N., Roland, M., Peichl, M., Migliavacca, M., Cremonese, E.,
556 Varlagin, A., Brümmer, C., La Gourlez de Motte, L., Fares, S., Buchmann, N., El-Madany, T. S.,
557 Pitacco, A., Vendrame, N., Li, Z., Vincke, C., Magliulo, E., and Koebisch, F.: Sensitivity of gross
558 primary productivity to climatic drivers during the summer drought of 2018 in Europe,
559 *Philosophical transactions of the Royal Society of London. Series B, Biological sciences*, 375,
560 20190747, <https://doi.org/10.1098/rstb.2019.0747>, 2020.

561 Fuchslueger, L., Bahn, M., Fritz, K., Hasibeder, R., and Richter, A.: Experimental drought reduces the
562 transfer of recently fixed plant carbon to soil microbes and alters the bacterial community
563 composition in a mountain meadow, *New Phytologist*, 201, 916–927,
564 <https://doi.org/10.1111/nph.12569>, 2014.

565 Fürst, J., Nachtnebel, H. P., Gasch, J., Nolz, R., Stockinger, M. P., Stumpp, C., and Schulz, K.: Rosalia:
566 an experimental research site to study hydrological processes in a forest catchment, *Earth Syst.
567 Sci. Data*, 13, 4019–4034, <https://doi.org/10.5194/essd-13-4019-2021>, 2021.

568 Fuss, R.: gasfluxes: greenhouse gas flux calculation from chamber measurements, 2020.

569 Futter, M. N., Dirnböck, T., Forsius, M., Bäck, J. K., Cools, N., Diaz-Pines, E., Dick, J., Gaube, V.,
570 Gillespie, L. M., Högbom, L., Laudon, H., Mirtl, M., Nikolaidis, N., Poppe Terán, C., Skiba, U.,
571 Vereecken, H., Villwock, H., Weldon, J., Wohner, C., and Alam, S. A.: Leveraging research

572 infrastructure co-location to evaluate constraints on terrestrial carbon cycling in northern
573 European forests, *Ambio*, 52, 1819–1831, <https://doi.org/10.1007/s13280-023-01930-4>, 2023.

574 Gartner, K. and Gollobich, G.: Klausen-Leopoldsdorf (Austria) - tree increments (2019-2021),
575 <https://doi.org/10.23728/B2SHARE.68D84A913F0C4875BE5C680AD4D6959E>, 2024.

576 Gartner, K., Gollobich, G., and Zolles, A.: Klausen-Leopoldsdorf (Austria) - meteorological data (2019-
577 2021), <https://doi.org/10.23728/B2SHARE.8F872A37513C4768B16CE755ECA4BB57>, 2024a.

578 Gartner, K., Gollobich, G., and Zolles, A.: Klausen-Leopoldsdorf (Austria) - soil temperature and soil
579 moisture (2019-2021),
580 <https://doi.org/10.23728/B2SHARE.8D49C0B557F1455A9E66689E035B8CCE>, 2024b.

581 Gillespie, L. M., Kolari, P., Kulmala, L., Leitner, S. M., Pihlatie, M., Zechmeister-Boltenstern, S., and
582 Díaz-Pinés, E.: Drought effects on soil greenhouse gas fluxes in a boreal and a temperate forest,
583 *Biogeochemistry*, 167, 155–175, <https://doi.org/10.1007/s10533-024-01126-2>, 2024.

584 Gillespie, L. M., Triches, N. Y., Abalos, D., Finke, P., Zechmeister-Boltenstern, S., Glatzel, S., and Díaz-
585 Pinés, E.: Land inclination controls CO₂ and N₂O fluxes, but not CH₄ uptake, in a temperate
586 upland forest soil, *SOIL*, 9, 517–531, <https://doi.org/10.5194/soil-9-517-2023>, 2023.

587 Glatzel, S., Worrall, F., Boothroyd, I. M., and Heckman, K.: Comparison of the transformation of
588 organic matter flux through a raised bog and a blanket bog, *Biogeochemistry*,
589 <https://doi.org/10.1007/s10533-023-01093-0>, 2023.

590 Gollob, C., Ritter, T., and Nothdurft, A.: Comparison of 3D Point Clouds Obtained by Terrestrial Laser
591 Scanning and Personal Laser Scanning on Forest Inventory Sample Plots, *Data*, 5, 103,
592 <https://doi.org/10.3390/data5040103>, 2020.

593 Grünzweig, J. M., Boeck, H. J. de, Rey, A., Santos, M. J., Adam, O., Bahn, M., Belnap, J., Deckmyn, G.,
594 Dekker, S. C., Flores, O., Gliksman, D., Helman, D., Hultine, K. R., Liu, L., Meron, E., Michael, Y.,
595 Sheffer, E., Throop, H. L., Tzuk, O., and Yakir, D.: Dryland mechanisms could widely control
596 ecosystem functioning in a drier and warmer world, *Nat Ecol Evol*, 6, 1064–1076,
597 <https://doi.org/10.1038/s41559-022-01779-y>, 2022.

598 Hartl-Meier, C., Zang, C., Büntgen, U., Esper, J., Rothe, A., Göttlein, A., Dirnböck, T., and Treydte, K.:
599 Uniform climate sensitivity in tree-ring stable isotopes across species and sites in a mid-latitude
600 temperate forest, *Tree Physiology*, <https://doi.org/10.1093/treephys/tpu096>, 2014.

601 Hasibeder, R., Fuchslueger, L., Richter, A., and Bahn, M.: Summer drought alters carbon allocation to
602 roots and root respiration in mountain grassland, *New Phytologist*, 205, 1117–1127,
603 <https://doi.org/10.1111/nph.13146>, 2015.

604 Haslinger, K., Bartsch, A.: Creating long-term gridded fields of reference evapotranspiration in Alpine
605 terrain based on a recalibrated Hargreaves method. *Hydrology and Earth System Sciences*, 20,
606 1211–1223, <https://hess.copernicus.org/articles/20/1211/2016/>, 2016.

607 Heimann, M. and Reichstein, M.: Terrestrial ecosystem carbon dynamics and climate feedbacks,
608 *Nature*, 451, 289–292, 2008.

609 Hutchinson, G. L. and Mosier, A. R.: Improved Soil Cover Method for Field Measurement of Nitrous
610 Oxide Fluxes, *Soil Sci. Soc. Am. j.*, 45, 311–316,
611 <https://doi.org/10.2136/sssaj1981.03615995004500020017x>, 1981.

612 Ingrisch, J. and Bahn, M.: Kaserstattalm (Austria) - forest soil CO₂ respiration (2019-2020),
613 <https://doi.org/10.23728/B2SHARE.CFE8C7AD1965433484650EA9026512CA>, 2024a.

614 Ingrisch, J. and Bahn, M.: Kaserstattalm (Austria) - forest tree increments (2019-2021),
615 <https://doi.org/10.23728/B2SHARE.0E3EED54FF30418F8720806B5F05CCA9>, 2024b.

616 Ingrisch, J. and Bahn, M.: Kaserstattalm (Austria) - meteorological data (2019-2021),
617 <https://doi.org/10.23728/B2SHARE.77462914DC0B43CB8C24A967E6851665>, 2024c.

618 Ingrisch, J. and Bahn, M.: Kaserstattalm (Austria) - soil temperature and soil moisture (2019-2021),
619 <https://doi.org/10.23728/B2SHARE.026D76094E8F4512B09B35B7A0D2A9D7>, 2024d.

620 Ingrisch, J. and Bahn, M.: Towards a Comparable Quantification of Resilience, *Trends in Ecology &*
621 *Evolution*, 33, 251–259, <https://doi.org/10.1016/j.tree.2018.01.013>, 2018.

622 Ingrisch, J., Karlowsky, S., Hasibeder, R., Gleixner, G., and Bahn, M.: Drought and recovery effects on
623 belowground respiration dynamics and the partitioning of recent carbon in managed and
624 abandoned grassland, *Glob Chang Biol*, 26, 4366–4378, <https://doi.org/10.1111/gcb.15131>, 2020.

625 Ingrisch, J., Karlowsky, S., Anadon-Rosell, A., Hasibeder, R., König, A., Augusti, A., Gleixner, G., and
626 Bahn, M.: Land Use Alters the Drought Responses of Productivity and CO₂ Fluxes in Mountain
627 Grassland, *Ecosystems*, 21, 689–703, <https://doi.org/10.1007/s10021-017-0178-0>, 2018.

628 IPCC: Climate Change 2021: The Physical Science Basis: Contribution of Working Group I to the Sixth
629 Assessment Report of the Intergovernmental Panel on Climate Change, Cambridge University
630 Press, Cambridge, United Kingdom and New York, NY, USA, 2021.

631 Kannenberg, S. A., Schwalm, C. R., and Anderegg, W. R. L.: Ghosts of the past: how drought legacy
632 effects shape forest functioning and carbon cycling, *Ecology Letters*, 23, 891–901,
633 <https://doi.org/10.1111/ele.13485>, 2020.

634 Kitzler, B., Zechmeister-Boltenstern, S., Holtermann, C., Skiba, U., and Butterbach-Bahl, K.: Controls
635 over N₂O, NO_x and CO₂ fluxes in a calcareous mountain forest soil, *Biogeosciences*, 3, 383–395,
636 2006.

637 Kitzler, B. and Hofbauer, A.: Klausen-Leopoldsdorf (Austria) - soil CO₂ respiration for the years (2019-
638 2020), <https://doi.org/10.23728/B2SHARE.5286BD1BC6AA491F874B9BB12D1C5673>, 2024.

639 Knierzinger, W., Drescher-Schneider, R., Knorr, K.-H., Drollinger, S., Limbeck, A., Brunnbauer, L.,
640 Horak, F., Festi, D., and Wagreich, M.: Anthropogenic and climate signals in late-Holocene peat
641 layers of an ombrotrophic bog in the Styrian Enns valley (Austrian Alps), *E&G Quaternary Sci. J.*,
642 69, 121–137, <https://doi.org/10.5194/egqsj-69-121-2020>, 2020.

643 Kobler, J., Dirnböck, T., and Pröll, G.: Zöbelboden (Austria) - meteorological data (2019-2021),
644 <https://doi.org/10.23728/B2SHARE.762E665273234B129D09EF017416BCFB>, 2024a.

645 Kobler, J., Dirnböck, T., and Pröll, G.: Zöbelboden (Austria) - soil CO₂ respiration for the years (2019-
646 2021), <https://doi.org/10.23728/B2SHARE.4F44006B932142E68981106A016F1F56>, 2024b.

647 Kobler, J., Dirnböck, T., and Pröll, G.: Zöbelboden (Austria) - soil temperature and soil moisture (2019-
648 2021), <https://doi.org/10.23728/B2SHARE.46E19191CE9C427D90F48CE38F56A0E1>, 2024c.

649 Kobler, J., Zehetgruber, B., Dirnböck, T., Jandl, R., Mirtl, M., and Schindlbacher, A.: Effects of aspect
650 and altitude on carbon cycling processes in a temperate mountain forest catchment, *Landscape*
651 *Ecol*, <https://doi.org/10.1007/s10980-019-00769-z>, 2019.

652 Kröel-Dulay, G., Mojzes, A., Szitár, K., Bahn, M., Batáry, P., Beier, C., Bilton, M., Boeck, H. J. de, Dukes,
653 J. S., Estiarte, M., Holub, P., Jentsch, A., Schmidt, I. K., Kreyling, J., Reinsch, S., Larsen, K. S.,
654 Sternberg, M., Tielbörger, K., Tietema, A., Vicca, S., and Peñuelas, J.: Field experiments
655 underestimate aboveground biomass response to drought, *Nature ecology & evolution*, 6, 540–
656 545, <https://doi.org/10.1038/s41559-022-01685-3>, 2022.

657 Kulmala, M.: Build a global Earth observatory, *Nature*, 553, 21–23, <https://doi.org/10.1038/d41586-017-08967-y>, 2018.

659 Leitner, S., Dirnböck, T., Kobler, J., and Zechmeister-Boltenstern, S.: Legacy effects of drought on
660 nitrate leaching in a temperate mixed forest on karst, *Journal of Environmental Management*,
661 262, <https://doi.org/10.1016/j.jenvman.2020.110338>, 2020.

662 Leitner, S., Minixhofer, P., Inselsbacher, E., Keiblinger, K. M., Zimmermann, M., and Zechmeister-
663 Boltenstern, S.: Short-term soil mineral and organic nitrogen fluxes during moderate and severe
664 drying–rewetting events, *Applied Soil Ecology*, 114, 28–33,
665 <https://doi.org/10.1016/j.apsoil.2017.02.014>, available at:
666 <https://www.sciencedirect.com/science/article/pii/S0929139316303018>, 2017.

667 LI-COR Biosciences: SoilFluxPro Software: Instruction manual, 2019.

668 Liu, D., Keiblinger, K. M., Leitner, S., Wegner, U., Zimmermann, M., Fuchs, S., Lassek, C., Riedel, K.,
669 and Zechmeister-Boltenstern, S.: Response of Microbial Communities and Their Metabolic
670 Functions to Drying–Rewetting Stress in a Temperate Forest Soil, *Microorganisms*, 7,
671 <https://doi.org/10.3390/microorganisms7050129>, 2019.

672 Mahecha, M. D., Gans, F., Sippel, S., Donges, J. F., Kaminski, T., Metzger, S., Migliavacca, M., Papale,
673 D., Rammig, A., and Zscheischler, J.: Detecting impacts of extreme events with ecological in situ
674 monitoring networks, *Biogeosciences*, 14, 4255–4277, <https://doi.org/10.5194/bg-14-4255-2017>,
675 2017.

676 Maier, A. and Glatzel, S.: Lake Neusiedl (Austria) - eddy flux data (2019–2021),
677 <https://doi.org/10.23728/B2SHARE.B83CACA3EFE44868A1ED49129B4A576A>, 2024a.

678 Maier, A. and Glatzel, S.: Lake Neusiedl (Austria) - meteorological data (2019–2021),
679 <https://doi.org/10.23728/B2SHARE.F7176C9EE982464F947D2FE9FB8F389D>, 2024b.

680 Maier, A. and Glatzel, S.: Lake Neusiedl (Austria) - soil temperature and soil moisture (2019–2021),
681 <https://doi.org/10.23728/B2SHARE.4E6474CD55F9487D97E3D31E83BAA530>, 2024c.

682 Maier, A. and Glatzel, S.: Puergschachen Bog (Austria) - eddy covariance data (2019–2021),
683 <https://doi.org/10.23728/B2SHARE.4F783E3FF2884ABCA5C59960DB0B7955>, 2024d.

684 Maier, A. and Glatzel, S.: Puergschachen Bog (Austria) - meteorological data (2019–2021),
685 <https://doi.org/10.23728/B2SHARE.5442510AD03E4968AFB4E2108E85A64D>, 2024e.

686 Maier, A. and Glatzel, S.: Puergschachen Bog (Austria) - soil temperature and soil moisture (2019–
687 2021), <https://doi.org/10.23728/B2SHARE.9380364098D14978B876A87517652D62>, 2024f.

688 Mirtl, M., T. Borer, E., Djukic, I., Forsius, M., Haubold, H., Hugo, W., Jourdan, J., Lindenmayer, D.,
689 McDowell, W. H., Muraoka, H., Orenstein, D. E., Pauw, J. C., Peterseil, J., Shibata, H., Wohner, C.,
690 Yu, X., and Haase, P.: Genesis, goals and achievements of Long-Term Ecological Research at the
691 global scale: A critical review of ILTER and future directions, *Science of The Total Environment*,
692 626, 1439–1462, <https://doi.org/10.1016/j.scitotenv.2017.12.001>, 2018.

693 Müller, L. M. and Bahn, M.: Drought legacies and ecosystem responses to subsequent drought, *Glob
694 Chang Biol*, 28, 5086–5103, <https://doi.org/10.1111/gcb.16270>, 2022.

695 Müller, R., Maier, A., Inselsbacher, E., Peticzka, R., Wang, G., and Glatzel, S.: ¹³C-Labeled Artificial
696 Root Exudates Are Immediately Respired in a Peat Mesocosm Study, *Diversity*, 14, 735,
697 <https://doi.org/10.3390/d14090735>, 2022.

698 Neumann, M. and Starlinger, F.: The significance of different indices for stand structure and diversity
699 in forests, *Forest Ecology and Management*, 145, 91–106, 2001.

700 Oberleitner, F., Hartmann, H., Hasibeder, R., Huang, J., Losso, A., Mayr, S., Oberhuber, W., Wieser, G.,
701 and Bahn, M.: Amplifying effects of recurrent drought on the dynamics of tree growth and water
702 use in a subalpine forest, *Plant, Cell & Environment*, 45, 2617–2635,
703 <https://doi.org/10.1111/pce.14369>, 2022.

704 Oggioni, A., Silver, M., Ranghetti, L., and Tagliolato, P.: ReLTER: An Interface for the eLTER
705 Community, <https://github.com/ropensci/ReLTER>, 2023.

706 Pröll, G., Venier, S., and Dirnböck, T.: Zöbelboden (Austria) - tree increments (2019–2021),
707 <https://doi.org/10.23728/B2SHARE.2DE5B37A0CAD4F82A19F477531D6AF24>, 2024.

708 Pumpanen, J., Kulmala, L., Lindén, A., Kolari, P., Nikinmaa, E., and Hari, P.: Seasonal dynamics of
709 autotrophic respiration in boreal forest soil estimated by continuous chamber measurements,
710 2015.

711 Pumpanen, J., Kolari, P., Ilvesniemi, H., Minkinen, K., Vesala, T., Niinistö, S., Lohila, A., Larmola, T.,
712 Morero, M., Pihlatie, M., Janssens, I., Yuste, J. C., Grünzweig, J. M., Reth, S., Subke, J.-A., Savage,
713 K., Kutsch, W., Østreg, G., Ziegler, W., Anthoni, P., Lindroth, A., and Hari, P.: Comparison of
714 different chamber techniques for measuring soil CO₂ efflux, *Agricultural and Forest Meteorology*,
715 123, 159–176, <https://doi.org/10.1016/j.agrformet.2003.12.001>, 2004.

716 Ramonet, M., Ciais, P., Apadula, F., Bartyzel, J., Bastos, A., Bergamaschi, P., Blanc, P. E., Brunner, D.,
717 Di Caracciolo Torchiarolo, L., Calzolari, F., Chen, H., Chmura, L., Colomb, A., Conil, S., Cristofanelli,
718 P., Cuevas, E., Curcoll, R., Delmotte, M., Di Sarra, A., Emmenegger, L., Forster, G., Frumau, A.,
719 Gerbig, C., Gheusi, F., Hammer, S., Haszpra, L., Hatakka, J., Hazan, L., Heliasz, M., Henne, S.,
720 Hensen, A., Hermansen, O., Keronen, P., Kivi, R., Komínková, K., Kubistin, D., Laurent, O., Laurila,
721 T., Lavric, J. V., Lehner, I., Lehtinen, K. E. J., Leskinen, A., Leuenberger, M., Levin, I., Lindauer, M.,
722 Lopez, M., Myhre, C. L., Mammarella, I., Manca, G., Manning, A., Marek, M. V., Marklund, P.,
723 Martin, D., Meinhardt, F., Mihalopoulos, N., Mölder, M., Morgui, J. A., Necki, J., O'Doherty, S.,
724 O'Dowd, C., Ottosson, M., Philippon, C., Piacentino, S., Pichon, J. M., Plass-Duelmer, C., Resovsky,
725 A., Rivier, L., Rodó, X., Sha, M. K., Scheeren, H. A., Sferlazzo, D., Spain, T. G., Stanley, K. M.,
726 Steinbacher, M., Trisolino, P., Vermeulen, A., Vítková, G., Weyrauch, D., Xueref-Remy, I., Yala, K.,
727 and Yver Kwok, C.: The fingerprint of the summer 2018 drought in Europe on ground-based
728 atmospheric CO₂ measurements, *Philosophical transactions of the Royal Society of London.*
729 *Series B, Biological sciences*, 375, 20190513, <https://doi.org/10.1098/rstb.2019.0513>, 2020.

730 Reichstein, M., Bahn, M., Ciais, P., Frank, D., Mahecha, M. D., Seneviratne, S. I., Zscheischler, J., Beer,
731 C., Buchmann, N., Frank, D. C., Papale, D., Rammig, A., Smith, P., Thonicke, K., van der Velde, M.,
732 Vicca, S., Walz, A., and Wattenbach, M.: Climate extremes and the carbon cycle, *Nature*, 500,
733 287–295, <https://doi.org/10.1038/nature12350>, 2013.

734 Rödenbeck, C., Zaehle, S., Keeling, R., and Heimann, M.: The European carbon cycle response to heat
735 and drought as seen from atmospheric CO₂ data for 1999–2018, *Philosophical transactions of the*
736 *Royal Society of London. Series B, Biological sciences*, 375, 20190506,
737 <https://doi.org/10.1098/rstb.2019.0506>, 2020.

738 Schindlbacher, A., Wunderlich, S., Borken, W., Kitzler, B., Zechmeister-Boltenstern, S., and Jandl, R.:
739 Soil respiration under climate change: prolonged summer drought offsets soil warming effects,
740 *Global Change Biology*, 18, 2270–2279, <https://doi.org/10.1111/j.1365-2486.2012.02696.x>, 2012.

741 Schmitt, M., Bahn, M., Wohlfahrt, G., Tappeiner, U., and Cernusca, A.: Land use affects the net
742 ecosystem CO₂ exchange and its components in mountain grasslands, *Biogeosciences*, 7, 2297–
743 2309, <https://doi.org/10.5194/bg-7-2297-2010>, 2010.

744 Schwen, A., Zimmermann, M., Leitner, S., and Woche, S. K.: Soil Water Repellency and its Impact on
745 Hydraulic Characteristics in a Beech Forest under Simulated Climate Change, *Vadose Zone*
746 *Journal*, 14, 1–11, <https://doi.org/10.2136/vzj2015.06.0089>, 2015.

747 Vicente-Serrano, S. M., Beguería S, and López-Moreno, J. I.: A Multiscalar Drought Index Sensitive to
748 Global Warming: The Standardized Precipitation Evapotranspiration Index, *Journal of Climate*, 23,
749 1696–1718, <https://doi.org/10.1175/2009JCLI2909.1>, 2010.

750 Wilkinson, M. D., Dumontier, M., Aalbersberg, I. J. J., Appleton, G., Axton, M., Baak, A., Blomberg, N.,
751 Boiten, J.-W., da Silva Santos, L. B., Bourne, P. E., Bouwman, J., Brookes, A. J., Clark, T., Crosas,
752 M., Dillo, I., Dumon, O., Edmunds, S., Evelo, C. T., Finkers, R., Gonzalez-Beltran, A., Gray, A. J. G.,
753 Groth, P., Goble, C., Grethe, J. S., Heringa, J., Hoen, P. A. C., Hooft, R., Kuhn, T., Kok, R., Kok, J.,
754 Lusher, S. J., Martone, M. E., Mons, A., Packer, A. L., Persson, B., Rocca-Serra, P., Roos, M., van
755 Schaik, R., Sansone, S.-A., Schultes, E., Sengstag, T., Slater, T., Strawn, G., Swertz, M. A.,
756 Thompson, M., van der Lei, J., van Mulligen, E., Velterop, J., Waagmeester, A., Wittenburg, P.,
757 Wolstencroft, K., Zhao, J., and Mons, B.: The FAIR Guiding Principles for scientific data
758 management and stewardship, *Scientific data*, 3, 160018, <https://doi.org/10.1038/sdata.2016.18>,
759 2016.

760 Wohner, C.: deimsPy, <https://pypi.org/project/deims/>, 2023.

761 Wohner, C., Peterseil, J., and Klug, H.: Designing and implementing a data model for describing
762 environmental monitoring and research sites, *Ecological Informatics*, 70, 101708,

763 <https://doi.org/10.1016/j.ecoinf.2022.101708>, available at:
764 <https://www.sciencedirect.com/science/article/pii/S1574954122001583>, 2022.

765 Wohner, C., Peterseil, J., Poursanidis, D., Kliment, T., Wilson, M., Mirtl, M., and Chrysoulakis, N.:
766 DEIMS-SDR – A web portal to document research sites and their associated data, *Ecological*
767 *Informatics*, 51, 15–24, <https://doi.org/10.1016/j.ecoinf.2019.01.005>, 2019.

768 Wohner, C., Dirnböck, T., Peterseil, J., Pröll, G., Geiger, S.: Providing high resolution data for the long-
769 term ecosystem research infrastructure on the national and European scale, in:
770 *Umweltinformationssysteme – Wie verändert die Digitalisierung unsere Gesellschaft?*, edited by:
771 Freitag, U., Fuchs-Kittowski, F., Abecker, A., Hosenfeld, F., Springer Vieweg, Wiesbaden, 2021.

772 Working Group WRB: World Reference Base for Soil Resources 2014, update 2015 International soil
773 classification system for naming soils and creating legends for soil maps, *World Soil Resources*
774 *Reports No. 106*. FAO, Rome, 2015.

775 Wu, D., Ciais, P., Viovy, N., Knapp, A. K., Wilcox, K., Bahn, M., Smith, M. D., Vicca, S., Fatichi, S.,
776 Zscheischler, J., He, Y., Li, X., Ito, A., ARNETH, A., Harper, A., Ukkola, A., Paschalis, A., Poulter, B.,
777 Peng, C., Ricciuto, D., Reinthaler, D., Chen, G., Tian, H., Genet, H., Mao, J., Ingrisch, J., Nabel, J. E.
778 S. M., Pongratz, J., Boysen, L. R., Kautz, M., Schmitt, M., Meir, P., Zhu, Q., Hasibeder, R., Sippel, S.,
779 Dangal, S. R. S., Sitch, S., Shi, X., Wang, Y., Luo, Y., Liu, Y., and Piao, S.: Asymmetric responses of
780 primary productivity to altered precipitation simulated by ecosystem models across three long-
781 term grassland sites, *Biogeosciences*, 15, 3421–3437, <https://doi.org/10.5194/bg-15-3421-2018>,
782 2018.

783 Yu, X., Orth, R., Reichstein, M., Bahn, M., Klosterhalfen, A., Knohl, A., Koebisch, F., Migliavacca, M.,
784 Mund, M., Nelson, J. A., Stocker, B. D., Walther, S., and Bastos, A.: Contrasting drought legacy
785 effects on gross primary productivity in a mixed versus pure beech forest, *Biogeosciences*, 19,
786 4315–4329, <https://doi.org/10.5194/bg-19-4315-2022>, 2022.

787 Zweifel, R.: Radial stem variations - a source of tree physiological information not fully exploited yet,
788 *Plant Cell and Environment*, 39, 231–232, <https://doi.org/10.1111/pce.12613>, 2016.

789 Zweifel, R., Pappas, C., Peters, R. L., Babst, F., Balanzategui, D., Basler, D., Bastos, A., Beloiu, M.,
790 Buchmann, N., Bose, A. K., Braun, S., Damm, A., D’Odorico, P., Eitel, J. U., Etzold, S., Fonti, P.,
791 Rouholahnejad Freund, E., Gessler, A., Haeni, M., Hoch, G., Kahmen, A., Körner, C., Krejza, J.,
792 Krumm, F., Leuchner, M., Leuschner, C., Lukovic, M., Martínez-Vilalta, J., Matula, R., Meesenburg,
793 H., Meir, P., Plichta, R., Poyatos, R., Rohner, B., Ruehr, N., Salomón, R. L., Scharnweber, T.,
794 Schaub, M., Steger, D. N., Steppe, K., Still, C., Stojanović, M., Trotsiuk, V., Vitasse, Y., Arx, G. von,
795 Wilmking, M., Zahnd, C., and Sterck, F.: Networking the forest infrastructure towards near real-
796 time monitoring – A white paper, *Science of The Total Environment*, 872, 162167,
797 <https://doi.org/10.1016/j.scitotenv.2023.162167>, 2023.

798 Zweifel, R., Etzold, S., Basler, D., Bischoff, R., Braun, S., Buchmann, N., Conedera, M., Fonti, P.,
799 Gessler, A., Haeni, M., Hoch, G., Kahmen, A., Köchli, R., Maeder, M., Nievergelt, D., Peter, M.,
800 Peters, R. L., Schaub, M., Trotsiuk, V., Walthert, L., Wilhelm, M., and Eugster, W.: TreeNet–The
801 Biological Drought and Growth Indicator Network, *Front. For. Glob. Change*, 4,
802 <https://doi.org/10.3389/ffgc.2021.776905>, 2021.

803